Earth and Planetary Science Letters 396 (2014) 97–106

Contents lists available at ScienceDirect

Earth and Planetary Science Letters

www.elsevier.com/locate/epsl

Phantom Archean crust in Mangaia hotspot lavas and the meaning of heterogeneous mantle

C. Herzberg [a,*], R.A. Cabral [b], M.G. Jackson [c], C. Vidito [a], J.M.D. Day [d], E.H. Hauri [e]

[a] Department of Earth and Planetary Sciences, Rutgers University, 610 Taylor Road, Piscataway, NJ 08854-8066, USA
[b] Boston University, Department of Earth and Environment, Boston, MA 02215, USA
[c] UC Santa Barbara, Department of Earth Science, Santa Barbara, CA 93106, USA
[d] Geosciences Research Division, Scripps Institution of Oceanography, La Jolla, CA 92093-0244, USA
[e] Department of Terrestrial Magnetism, Carnegie Institution of Washington, Washington, DC 20015, USA

ARTICLE INFO

Article history:
Received 30 July 2013
Received in revised form 24 January 2014
Accepted 31 March 2014
Available online xxxx
Editor: T. Elliott

Keywords:
olivine
peridotite
pyroxenite
eclogite
isotopes
HIMU

ABSTRACT

Lavas from Mangaia in the Cook–Austral island chain, Polynesia, define an HIMU (or high μ, where $\mu = {}^{238}U/{}^{204}Pb$) global isotopic end-member among ocean island basalts (OIB) with the highest ${}^{206,207,208}Pb/{}^{204}Pb$. This geochemical signature is interpreted to reflect a recycled oceanic crust component in the mantle source. Mass independently fractionated (MIF) sulfur isotopes indicate that Mangaia lavas sampled recycled Archean material that was once at the Earth's surface, likely hydrothermally-modified oceanic crust. Recent models have proposed that crust that is subducted and then returned to the surface in a mantle plume is expected to transform to pyroxenite/eclogite during transit through the mantle. Here we examine this hypothesis for Mangaia using high-precision electron microprobe analysis on olivine phenocrysts. Contrary to expectations of a crustal component and, hence pyroxenite, results show a mixed peridotite and pyroxenite source, with peridotite dominating. If the isotopic compositions were inherited from subduction of recycled oceanic crust, our work shows that this source has phantom-like properties in that it can have its lithological identity destroyed while its isotope ratios are preserved. This may occur by partial melting of the pyroxenite and injection of its silicic melts into the surrounding mantle peridotite, yielding a refertilized peridotite. Evidence from one sample reveals that not all pyroxenite in the melting region was destroyed. Identification of source lithology using olivine phenocryst chemistry can be further compromised by magma chamber fractional crystallization, recharge, and mixing. We conclude that the commonly used terms mantle "heterogeneities" and "streaks" are ambiguous, and distinction should be made of its lithological and isotopic properties.

1. Introduction

Oceanic plates, including crust and mantle lithosphere, enter the mantle at subduction zones. Integrated over geologic time, subduction of oceanic crust has generated a large reservoir of crustal material that must now reside in the Earth's mantle. Regions of buoyantly upwelling mantle, called mantle plumes, are thought to return some of the crustal material to the shallow mantle, where it melts and is erupted at hotspots (Morgan, 1971; Hofmann and White, 1982; White and Hofmann, 1982). In order to evaluate this hypothesis for deep recycling, it is important to detect petrological and geochemical signatures of ancient subducted materials in hotspot lavas.

Lavas from the island of Mangaia, located in the Cook Islands, have the most radiogenic Pb isotope compositions amongst OIB globally (Hauri and Hart, 1993; Woodhead, 1996; Chauvel et al., 1997). This isotopic signature, together with trace element compositions, has been interpreted to reflect a recycled oceanic crust component in the mantle source of Mangaia lavas (Zindler and Hart, 1986; Chauvel et al., 1992, 1995; Hauri and Hart, 1993; Hofmann, 1997; Weaver, 1991; Willbold and Stracke, 2006). Supporting this hypothesis, MIF sulfur isotope signatures, which were uniquely generated in the Earth's atmosphere in the Archean, were recently discovered in olivine-hosted sulfide inclusions from Mangaia lavas (Cabral et al., 2013). This signature provides the strongest evidence yet for deep recycling of surface materials into the mantle source of hotspot lavas. Armed with this evidence for deep recycling – from subduction zones to mantle plumes – it is important to characterize the present-day mantle that sourced Mangaia lavas.

* Tel.: +1 (848) 445 3154; fax: +1 (732) 445 3374.
E-mail address: Herzberg@rci.rutgers.edu (C. Herzberg).

http://dx.doi.org/10.1016/j.epsl.2014.03.065
0012-821X/

The Pb isotope ratios that characterize the HIMU component in OIB must involve a process that strongly fractionates U/Pb and Th/Pb ratios. Loss of Pb during subduction-driven dewatering of the oceanic crust is one such process (Chauvel et al., 1992, 1995; Hofmann, 1997; Kelley et al., 2005). OIB that sample a region of the mantle with subducted crust, preserved as pyroxenite/eclogite, are expected to crystallize olivine with high Ni, low Ca, low Mn and high Fe/Mn compared to melts of peridotite (Sobolev et al., 2005, 2007; Gurenko et al., 2009, 2010; Herzberg, 2011), and may also be expressed in terms of distinctive trace-element and isotope systematics (Gurenko et al., 2009; Day et al., 2009, 2010; Day and Hilton, 2011). An important question, therefore, is whether HIMU lavas, which sample recycled oceanic crust, crystallize olivine that implicates a pyroxenite protolith.

While recycled crust may contribute to the HIMU component in OIB, it may not be expressed as a distinct pyroxenite lithology. Recycled crust that is mixed into its host peridotite during convective stirring might produce a fertilized peridotite (Jackson et al., 2008; Gurenko et al., 2009; Parai et al., 2009). Understanding the source lithology of HIMU magmas can therefore place constraints on the long-term involvement of recycled crust, whether it is direct in the form of pyroxenite melting beneath a hotspot or indirect in the form of peridotite melting. In principle, inferences about source lithology are now a tractable problem using the composition of olivine phenocrysts as a tracer. Using olivine phenocryst compositions, we draw first-order conclusions about the source lithology of the HIMU isotopic reservoir using samples from Mangaia, the HIMU type locality, but identify areas where petrological interpretations are compromised and non-unique. We discuss implications for the preservation of recycled crust as a pyroxenite lithology in the mantle.

2. Samples, analytical methods and results

Five lavas from the island of Mangaia were examined in this study, and they are all porphyritic olivine- and clinopyroxene-bearing alkali basalts. Two of the lavas, MGA-B-25 and MGA-B-47, were collected in the 1990 field season and were previously characterized geochemically by Hauri and Hart (1993, 1997), and both host MIF sulfur anomalies (Cabral et al., 2013). Point counting of phenocrysts in petrographic thin sections reveals about 20% olivine and 20% clinopyroxene in MGA-B-25, and about 60% olivine and 10% clinopyroxene in MGA-B-47. New samples were collected during a field campaign in 2010, and they have the following phenocryst modes: MG-1001 (40% olivine and 10% clinopyroxene), MG-1002 (20% olivine and 30% clinopyroxene), and MG-1006 (20% olivine and 10% clinopyroxene). Additionally, all samples contain opaque phases, most likely as chrome-rich spinels as revealed in positive correlations of whole rock MgO–Cr_2O_3.

Whole rock data are given in Table A1 in the Online Appendix. Major and select trace element (Sc, V, Cr, Co, Ni, Cu, Zn, Ga, Rb, Sr, Y, Zr, Nb, Ba, La, Ce, Pb, U, and Th) compositions for samples MG-1001, MG-1002, and MG01006 were measured by XRF at Franklin and Marshall College using a *PW 2404 PANalytical XRF* vacuum spectrometer following the procedures outlined in Boyd and Mertzman (1987). Briefly, major element analyses by XRF involved standard lithium tetraborate fusion techniques using 3.6:0.4 g $LiBO_4$:sample powder. Ferrous iron concentrations were determined by titration with potassium dichromate. Trace element analyses involved standard copolywax preparation (7 g powder: 1.4 g copolywax). Additional details of analytical methods are given at http://www.fandm.edu/earth-and-environment/major-element-technique. Whole rock data for MG-B-47 is given in Hauri and Hart (1997). Whole rock data for MG-B-25 are unreliable because this sample is heavily altered.

We analyzed olivine phenocrysts in seven samples from Mangaia. A total of 316 high precision analyses were obtained from olivine phenocrysts of varying sizes and forsterite contents. Single core analyses were taken from olivine phenocrysts identified as homogeneous from backscatter images. Traverses were taken from olivines that exhibited zoning.

Olivine, major element, and trace element data were obtained using a slightly modified method of Sobolev et al. (2007). Analyses were conducted on the Jeol JXA-8200 electron microprobe at Rutgers University. A current of 300 nA and an accelerating voltage of 20 kV were used for all analyses. Count times on the elements are as follows: 50 s for Si, 80 s for Mg, 100 s for Fe, and 150 s for Mn, Ni, and Ca. We calibrated on synthetic fayalite or tephroite for Si; synthetic forsterite for Mg; synthetic fayalite for Fe; synthetic tephroite for Mn; synthetic Ni_2SiO_2 or SRM 126c (36% Ni) for Ni and Kakanui Augite (USNM 122142) for Ca. We used a San Carlos olivine standard only for drift correction, and it was analyzed at regular intervals throughout every run. Detection limits at a 3σ (99%) confidence level and errors (2σ) were obtained from the Probe for EPMA program (Donovan, 2012). Average detection limits for Si, Mg, and Fe are 30, 22 and 32 ppm, respectively. Average detection limits for trace elements Ni, Mn, and Ca are 23, 22, and 19 ppm, respectively. Analyses of major elements Si, Mg, and Fe have an average relative 2σ error of $\sim$0.09%, $\sim$0.09%, and $\sim$0.18% respectively. Average 2σ errors for trace elements Ni, Mn, and Ca are 25 ppm, 31 ppm, and 33 ppm respectively. 2 standard deviations of Ni, Mn, Ca and Fo# for the San Carlos olivine analyses ($n = 97$) in our study are 57 ppm, 31 ppm, 19 ppm and 0.1% respectively. Analyses with oxide totals greater than $\pm$2% deviation from 100% were excluded. Chemical formulas were calculated for all analyses. Analyses with deviations in stoichiometry greater than $\pm$1% were excluded.

Olivine compositions are shown in Fig. 1 for MG-1001, MG-1002, MGA-B-25 and MGA-B-47; they are homogeneous or they display modest normal zoning, with Mg-numbers decreasing from the cores to rims. All data are individual analyses with no averaging. Results for MG-1006 are more complex in that they contain olivines with both normal and reverse zoning, and they will be discussed separately in Section 6 below.

3. Petrological modeling

Our goal is to use high precision olivine data shown in Fig. 1 to infer the lithology of the source that melted to produce the Mangaia lavas. When olivine Mg-numbers are greater than 90, pyroxenite sources are often revealed in olivine phenocrysts with high Ni, low Ca, low Mn and high Fe/Mn compared to olivines that crystallize from melts of peridotite (Sobolev et al., 2005, 2007; Gurenko et al., 2009, 2010; Herzberg, 2011). For example, olivine in mantle peridotite from a wide range of tectonic environments typically contain $\sim$3000 ppm Ni (Herzberg et al., 2013); these are similar to olivine in primitive MORB from the East Pacific Rise and olivines that have been inferred to have crystallized from primary magmas of Archean komatiites (Herzberg, 2011; Herzberg et al., 2013). The inference of source lithology becomes more challenging when interpreting olivine phenocrysts with Mg numbers $<$90, like those from Mangaia (i.e., 79–86; Fig. 1). For example, extraction of heat from a peridotite-source primary magma can be accomplished by fractional crystallization of both olivine and clinopyroxene. When clinopyroxene participates, the derivative magma will be relatively enriched in Ni and depleted in Ca and Mn (Herzberg et al., 2013; Vidito et al., 2013). Olivines that crystallize from such derivative magmas will also be relatively enriched in Ni and depleted in Ca and Mn, a signal that might be confused with a pyroxene-rich source. For Mangaia, the case for clinopyroxene crystallization is obvious in their observed phenocrysts, and the effects of fractional

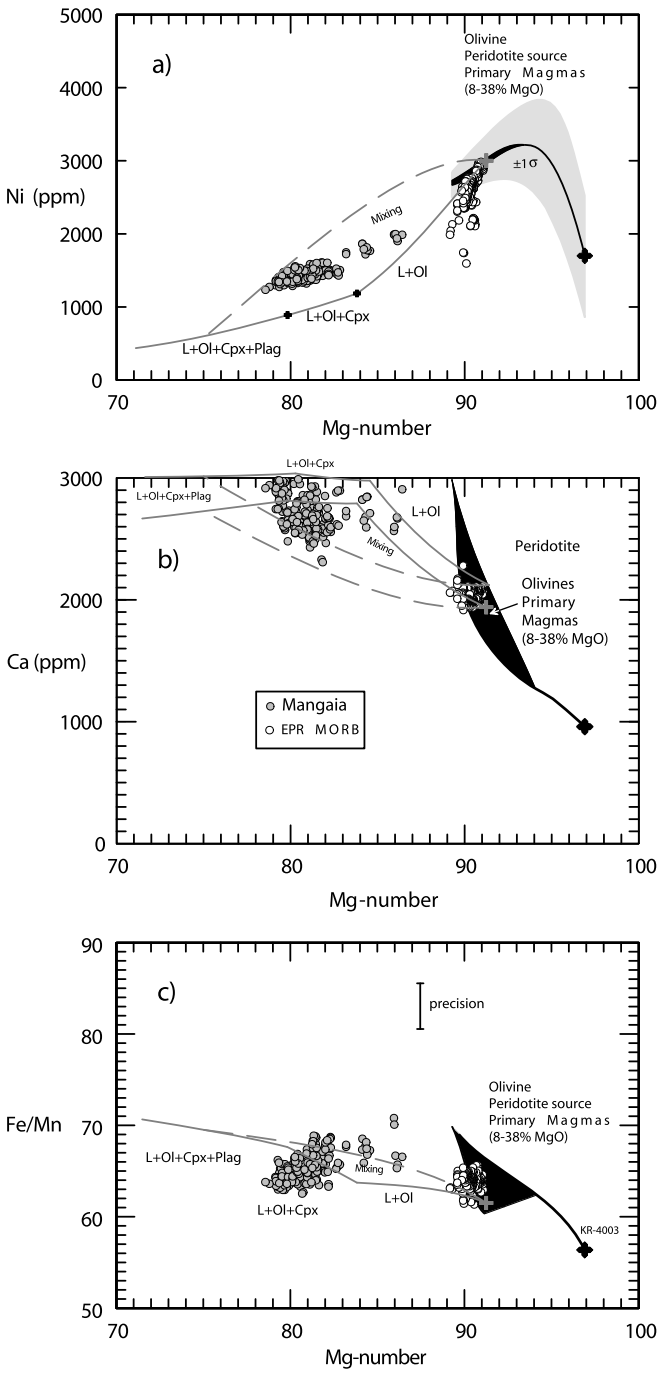

Fig. 1. Mg-numbers versus Ni and Ca contents and Fe/Mn for calculated (Herzberg, 2011) and observed olivine. An Mg-number is defined as 100MgO/(MgO + FeO) in mole per cent. Black forms = calculated Ni and Ca in olivines that crystallize from all primary melts derived from a fertile peridotite source having 1960 ppm Ni, 3.45% CaO and 0.13% MnO (Herzberg, 2011); the grey field in panel a represents $\pm 1\sigma$ uncertainty for Ni (Herzberg et al., 2013). The solid gray lines are olivine compositions that crystallize from an assumed Mangaia primary magma that subsequently fractionated olivine, clinopyroxene and plagioclase at 0.2 GPa, an olivine liquid line of descent (OLLD). The broken lines are olivines that would crystallize from mixed magmas given in Fig. 2. The fields bounded by the broken lines and OLLD simulate the range of olivine compositions that would crystallize by magma chamber fractional crystallization, recharge, and mixing. Mangaia olivines are from samples MGA-B-25, MGA-B-47, MG-1001, MG-1002, normalized to 100%. Precision in Ca and Ni is about the size of the symbols. Small variations in Mn propagate to significant variations in Fe/Mn as represented by the bracket. Olivines from the East Pacific Rise MORB are from Sobolev et al. (2007). Fe/Mn is a ppm ratio.

crystallization must be evaluated in order to draw conclusions about the mantle source (O'Hara, 1968), which involves petrological modeling. We assume that clinopyroxene crystallized in a shallow magma chamber below Mangaia, but acknowledge that it can occur in the mantle (O'Hara, 1968; Albarède et al., 1997; Geist et al., 1998; Herzberg and Asimow, 2008; Herzberg et al., 2013; Vidito et al., 2013). An evaluation of where, exactly, clinopyroxene fractionation occurs in OIB petrogenesis requires detail modeling that is beyond the scope of this paper.

A detailed description of the method we adopt for petrological modeling was provided previously (Herzberg, 2011; Herzberg et al., 2013), and is given again here in a somewhat abbreviated form. The petrological model has the following components: 1) identification of a primary magma composition, 2) calculation of a liquid line of descent after variable proportions of olivine, clinopyroxene and plagioclase have been subtracted, 3) calculation of the compositions of olivine that crystallize from these derivative magmas, 4) comparison of model and observed olivine compositions.

3.1. Mangaia primary magma composition

Primary magma compositions for peridotite-sources have been computed from primitive lava compositions using PRIMELT2 (Herzberg and Asimow, 2008) and results for lavas from the Cook–Austral Islands were reported earlier (Herzberg and Asimow, 2008; Herzberg and Gazel, 2009). However, successful solutions for Mangaia could not be obtained because the published lava database is limited. Furthermore, implementation of PRIMELT2 inverts the effects of fractional crystallization of olivine in order to restore primary magma composition (Herzberg and O'Hara, 2002), and the method is restricted to primitive lavas and glasses that gained or lost only olivine. This excludes Mangaia lavas because of their substantial content of clinopyroxene phenocrysts, and we know of no method that reliably inverts clinopyroxene crystallization because crystal sorting can yield considerable variation in phenocryst mode. Furthermore, we will show that the olivine phenocryst compositions are consistent with magma chamber dynamics that include fractional crystallization, recharge and mixing, processes that rule out the possibility of properly restoring primary magma composition.

Given that an inverse model is not tractable for Mangaia, a forward model strategy is adopted that assumes a peridotite-source primary magma composition. We begin by identifying a glass produced in experiment 40.06 by Walter (1998) on fertile peridotite KR-4003 as our assumed Mangaia peridotite-source primary magma composition. This particular composition was chosen because, as discussed below, its derivative melts crystallize olivines with compositions that have many similarities to Mangaia olivines. The experiment was run at 4 GPa and 1590 °C, the residuum mineralogy is olivine + clinopyroxene + garnet, the glass contains 18.58% MgO and it was produced by 9.2% equilibrium melting of peridotite (Walter, 1998). It is understood that the exact matching of Mangaia's primary magma with any experimental melt is unlikely for many reasons. We will show that Walter's melt composition is slightly low in CaO and TiO_2, most likely because it does not capture contributions from recycled crust (Dasgupta et al., 2007; Prytulak and Elliott, 2007). Walter did not report Ni in his experiments, so we assumed the Ni content using Ni (ppm) = 21.6 MgO − $0.32MgO_2$ + $0.051MgO_3$ for a peridotite source (Herzberg, 2011). However, Walter's melt 40.06 is very similar in composition to a successful PRIMELT2 solution listed in Herzberg and Gazel (2009) for basalt sample RRT-B-21 from Rurutu in the Cook–Austral chain (Hauri and Hart, 1997), which is similarly high in MgO (18.8%) and exhibits an HIMU flavor. A successful PRIMELT2 solution was also obtained for one sample from Tubuaii which is located closer to Mangaia and for which 16.4% MgO was obtained

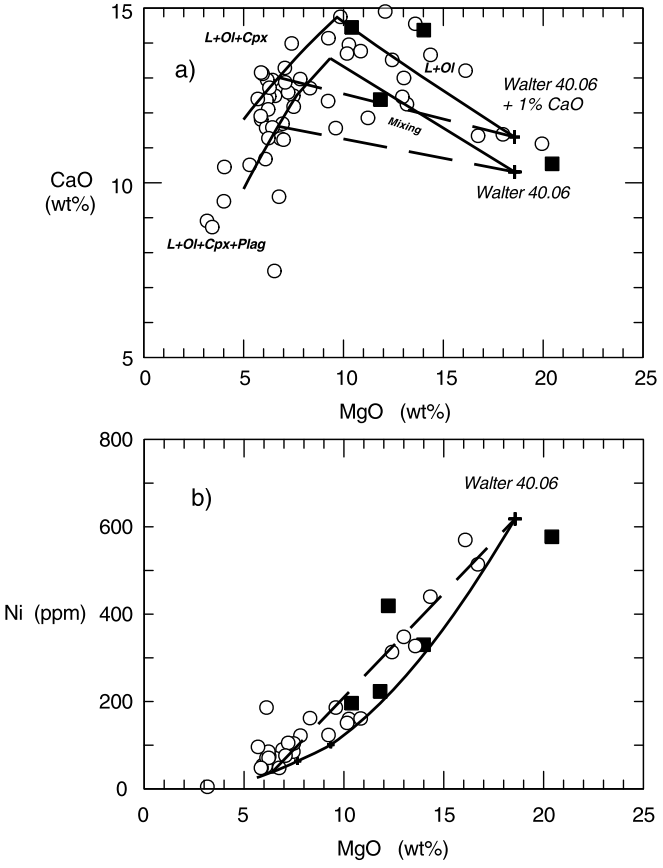

Fig. 2. A model for fractional crystallization of a Mangaia primary magma, recharge and mixing in a magma chamber at 0.2 GPa. Black lines are computed liquid lines of descent (LLD) using PETROLOG (Danyushevsky and Plechov, 2011) on a Mangaia primary magma that is assumed to have the compositions of Walter's (1998) 40.06 experimental composition, modified also by 1% CaO addition. Walter's melt composition was performed on fertile peridotite KR-4003. Broken lines are mixed end-members that, together with the LLD, provide bounds on the fields of mixed magmas. Whole rock analyses for lavas from Mangaia: open circles are compiled whole rock compositions compiled from Mangaia (Wood, 1978; Woodhead, 1996; Dupuy et al., 1989; Kogiso et al., 1997; Hauri and Hart, 1993, 1997); black squares are new whole rock data for MG-1001, -1002, and -1006 reported in this paper (Table A1 in the Online Appendix) and MGA-B-47 reported by Hauri and Hart (1997); analysis MGA-B-25 (Hauri and Hart, 1993) plots off scale in the upper panel and is unreliable owing to extensive alteration.

for the primary magma; however, this solution yielded model olivine compositions that were much lower in Ni and higher in Fe/Mn than observed Mangaia olivines.

3.2. Liquid line of descent (LLD)

We assumed that fractional crystallization of our primary magma occurred strictly in a shallow magma chamber at 0.2 GPa, and computed the liquid line of descent using PETROLOG (Danyushevsky and Plechov, 2011). To keep the LLD geochemically faithful to Walter's experimental melt composition, we assumed that crystallization was anhydrous and with all iron as FeO; evidence was presented for a role played by ~1% H_2O in OIB (Herzberg and Asimow, 2008), but this amount will not significantly affect the LLD. We assume partitioning models developed by Danyushevsky (2001) for clinopyroxene, plagioclase and melt. Olivine is the liquids phase, and it is followed by clinopyroxene and plagioclase, a result that is also obtained using pMELTS (Ghiorso et al., 2002). Clinopyroxene dominates over olivine when it begins to crystallize, and this is revealed by a break in the LLD for CaO and Ni at MgO below 10 wt.% (Fig. 2). PETROLOG permits the user to input the olivine/melt distribution coefficients for Ni

Table 1
Olivine/liquid Ni partition (D) models & their uncertainties.

Model	RMSE
Beattie et al. (1991)	1.1
Li and Ripley (2010)	1.4
Putirka et al. (2011; Eq. 2a)	2.7
Putirka et al. (2011; Eq. 2b)	2.0
Putirka et al. (2011; Eq. 2c)	2.9
Matzen et al. (2013)	2.5
Hart and Davis (1978)	4.2
Niu et al. (2011)[a]	2.1

RMSE = Root Mean Square Error. 1 RMSE = $(\sum(\text{model } D\ \text{Ni} - \text{experimental } D\ \text{Ni})^2/N)^{0.5}$. $N = 271$ FeO-bearing experiments listed in Herzberg et al. (2013) together with 13 experiments in Matzen et al. (2013).
[a] Does not include data at 1 atmosphere.

(D_{Ni}), and we have chosen the Beattie–Jones model (Jones, 1984; Beattie et al., 1991) because it provides consistency with previous work (Herzberg, 2011; Herzberg et al., 2013). There are other olivine/liquid distribution models (Hart and Davis, 1978; Li and Ripley, 2010; Putirka et al., 2011; Niu et al., 2011; Matzen et al., 2013), and all are parameterizations of experimental data. But the Beattie–Jones model has the minimum root mean square error (Table 1), and it is the most accurate. We assumed no Ni in plagioclase. For clinopyroxene and liquid, we assumed D_{Ni} varies with the composition of the liquid (Herzberg et al., 2013; Supplementary Information), yielding D values that are in good agreement with experimental measurements of Le Roux et al. (2011). PETROLOG describes the relative masses of crystallizing olivine, clinopyroxene, and plagioclase, information that we use to compute bulk partition coefficients along an LLD from mineral distribution coefficients.

3.3. Olivines on the liquid line of descent (OLLD)

The compositions of olivine that crystallizes along the liquid line of descent (OLLD) were calculated for Ni using the Beattie-Jones model and for Ca and Mn using distribution coefficients reported in Herzberg and O'Hara (2002).

3.4. Comparison of model and observed olivine compositions

Model olivine compositions on the liquid line of descent are now compared with observed olivine compositions for MG-1001, MG-1002, MGA-B-25 and MGA-B-47. As mention above, results for MG-1006 differ and they will be discussed separately.

4. Model results and evidence for peridotite in the mantle source for Mangaia

Fig. 1 illustrates that, within the precision of measurement, Fe/Mn in observed olivines are well-matched with model olivines as well as those that have been measured from East Pacific Rise MORB for which a peridotite source has been inferred (Sobolev et al., 2007; Herzberg, 2011). However, observed olivines differ from model olivines on the liquid line of descent in having higher Ni and lower Ca at any given Mg-number. And like Mangaia, work on MORB reveals that their geochemistry also cannot be explained solely by fractional crystallization, but must include recharge of the magma chamber with primary magma and subsequent mixing with liquid on the LLD (O'Hara, 1977; O'Neill and Jenner, 2012). We now include magma chamber recharge of our primary magma and mixing with liquids on the LLD (Fig. 2), and calculate the olivine compositions that would crystallize from these new liquid compositions. The broken line in Fig. 1 represents one end-member mixing solution whereby a derivative liquid with 6.75% MgO is

mixed with a new batch of primary magma that recharges the magma chamber (Fig. 2). The olivine field bounded by the OLLD and olivines that crystallize from the end-member mixing solution defines a wide range of mixing possibilities, and provides a good match to observed olivines (Fig. 1). While the calculation was made to produce an optimum match, it may be no coincidence that lavas from the Cook–Austral chain also have maximum FeO contents at around 6% MgO, dropping at lower MgO contents owing to magnetite fractionation. Application of PETROLOG to our primary magma, modified for an oxygen fugacity at the QFM buffer, and calculation of magma density (Lange and Carmichael, 1987) along the LLD reveals the production of FeO-rich liquids with maximum densities at around 6% MgO. Such derivative liquids may have settled to the magma chamber floor where they were exposed to and mix with subsequent batches of primary melt.

The Ca contents of observed olivines are generally higher than model olivines that crystallize from either the LLD or mixed magmas (Fig. 1). This misfit likely arises because the CaO content of our assumed Mangaia primary magma is too low. A better result is obtained by increasing CaO in Walter's experimental composition a small amount, from 10.31 to 11.31% (Figs. 1, 2). It is possible that a carbonated peridotite might be a better source because its partial melts are higher in CaO than volatile-free peridotite (Dasgupta et al., 2007) and Mangaia lavas are CO_2 rich, as evidenced by the presence of carbonatite blebs in olivine-hosted inclusions from Mangaia (Saal et al., 1998). Primitive high-Mg lavas from the Cook–Austral chain consist of a wide range of compositions from basalts having ~48% SiO_2 to nephelinites with 38% SiO_2. The lavas display negative SiO_2–CaO correlations, indicating they are related by partial melting of a carbonated peridotite source (Dasgupta et al., 2007). However, the lavas have higher alkalis than the experimental melts of Dasgupta et al. (2007) and negative SiO_2–La/Yb correlations, a difference that might be attributed to refertilization or metasomatism of a peridotite source from recycled crust (Jackson and Dasgupta, 2008).

The most important conclusion drawn from petrological modeling is that the Mangaia lavas are reasonably well-described by a model that involves a peridotite source, and one that was likely carbonated. Fractional crystallization of the Mangaia primary magma occurred in a shallow magma chamber which was replenished by subsequent batches of primary magma. A model of magma mixing and crystallization yields olivines that are a good match with observed olivine compositions. We now evaluate whether this peridotite source model is unique.

5. Evidence for refertilized peridotite in the mantle source for Mangaia

The evidence from olivine of a peridotite source for Mangaia appears to be at odds with isotopic evidence for a role played by recycled crust. We now seek a resolution to this paradox by examining prior hypotheses for the origin of a peridotite source for HIMU lavas from the Canary Islands (Gurenko et al., 2009, 2010; Day et al., 2009, 2010). While there is no compelling reason to assume the sources of Mangaia and the Canary Islands were identical, it is worth noting that the models for the latter differ in details that may be relevant to the present discussion.

Gurenko et al. (2009, 2010) form HIMU peridotite by mixing of recycled crust into peridotite, similar to that proposed by Parai et al. (2009) for the Cook–Austral Islands. Based on Pb–Os isotope systematics Hauri and Hart (1993) estimated an HIMU Mangaia source as a basalt–peridotite mixture, the proportions of which depend on the age of the crust (~20% for ancient basaltic crust). Day et al. (2009, 2010) and Hanyu et al. (2011) propose a mixed peridotite-pyroxenite source, partial melting of the recycled crust, and metasomatic injection and reaction of the melts into the host peridotite in order to comply with the severe constraints on total crustal source material imposed by Os isotopes. This model was originally proposed from a petrological view by Yaxley and Green (1998) who showed that recycled basaltic crust can partially melt at 3 GPa to yield dacite, an experimental observation that has been reproduced (Pertermann and Hirschmann, 2003; Spandler et al., 2008). At 3 GPa, SiO_2-rich melts of quartz eclogite have been observed to react with the peridotite host to produce orthopyroxene-rich layers (Yaxley and Green, 1998); if such melts percolate into the peridotite, they may react out of existence, forming a solid refertilized peridotite enriched in orthopyroxene, clinopyroxene and garnet (Yaxley and Green, 1998). This process was examined experimentally by Mallik and Dasgupta (2012, 2013) who showed that the infiltrating melts can evolve to silica-deficient compositions. In nature, whether dacitic melts produce layers of pyroxenite or refertilized peridotite will likely depend on the mode of melt transport; porous flow is expected to yield refertilized peridotite whereas pyroxenite is likely to be produced by channel flow. Evidence for production of pyroxenite veins by peridotite–dacite melt has been documented in mantle xenoliths (Liu et al., 2005). Prytulak and Elliott (2009) suggested that peridotite refertilized by dacitic melts might be an ideal way to reconcile the low melt productivity of Pico Island in the Azores as inferred from ^{238}U–^{230}Th and ^{235}U–^{231}Pa disequilibria with the geochemical evidence for involvement of recycled crust. Furthermore, evidence for peridotite refertilization by melts of pyroxenite has been documented in orogenic peridotite (Marchesi et al., 2013). The essential question is whether olivine phenocryst compositions can be used to distinguish partial melts of fertilized peridotite or pyroxenite. Sobolev et al. (2005, 2007) and later Herzberg (2011) proposed that partial melts of olivine-free pyroxenites will crystallize olivines in Hawaii with elevated Ni and low Ca and Mn. But how do such olivines compare with those that crystallize from partial melts of refertilized peridotite? We now examine this model computationally because there presently exist no high precision olivine data on experimental melts of fertilized peridotite appropriate to Mangaia.

The model setup is similar to that which was described previously (Herzberg and O'Hara, 2002; Herzberg, 2011), and consists of the following components: 1) a dacite melt composition A200K from Pertermann and Hirschmann (2003) is mixed with peridotite KR-4003 in 10 wt% increments to yield a variety of source compositions that range from refertilized peridotite to pyroxenite; Ni contents were not measured, so we calculated it assuming the dacite is in equilibrium with mantle olivine having 0.36% NiO, similar to that described by Wang and Gaetani (2008); 2) the compositions of liquids extracted from residues of olivine and olivine + orthopyroxene were computed by mass balance solutions to the equation for accumulated fractional melting using bulk distribution coefficients derived from distribution coefficients of olivine and orthopyroxene weighted in variable proportions in the peridotite-dacite mixes; 3) olivine phenocryst compositions are computed as described above for olivines that crystallize along a liquid line of descent at 0.2 GPa. We emphasize that the model has its limitations because residual clinopyroxene and garnet have not been included owing to the added computational complexity. Nevertheless, it provides a bound on the possible olivine compositions and the effects of residual clinopyroxene and garnet can be estimated qualitatively; below we indicate the role these phases play in modifying the Ni, Fe/Mn and Ca of magmatic olivines. Results are shown in Fig. 3.

When increasing amounts of dacite are added to peridotite, the partial melts crystallize olivines with increasing Ni, decreasing Ca, and increasing Fe/Mn (Fig. 3). For Ni, the effect is similar to that explored by Kelemen et al. (1998) wherein Ni-rich melts in equilibrium with orthopyroxene are produced by the reaction of a

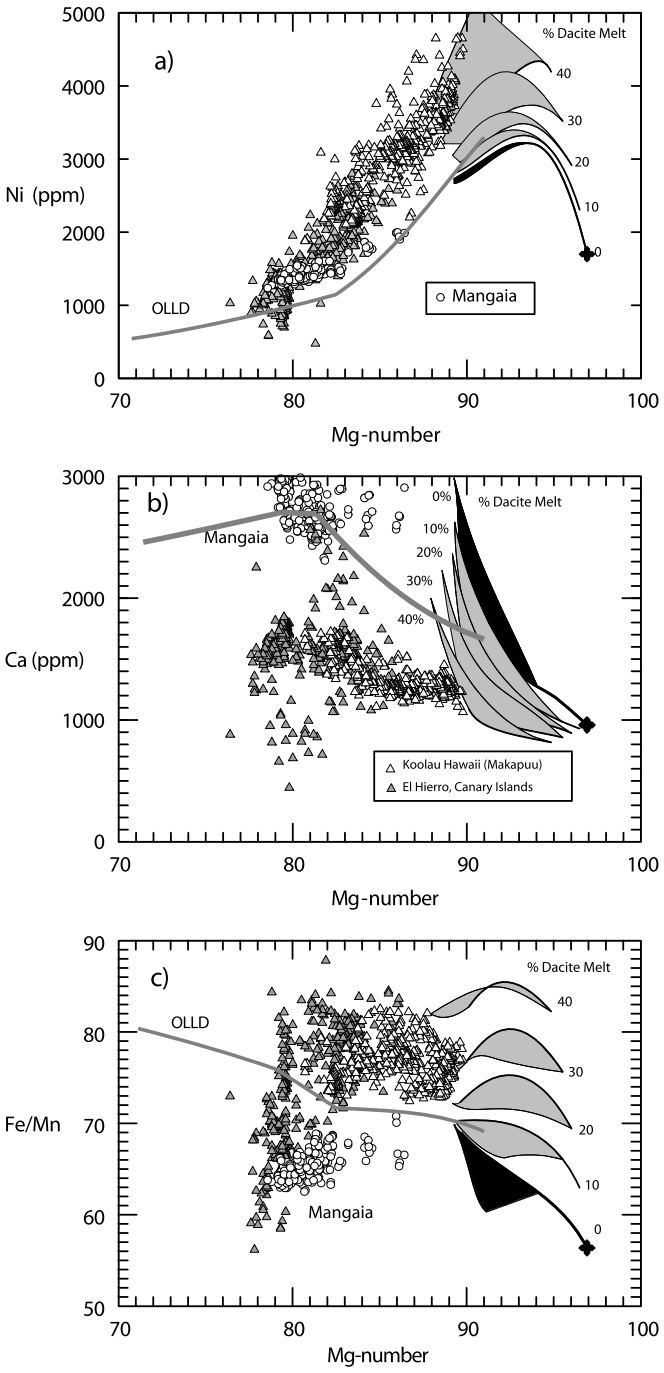

Fig. 3. A model of olivine compositions that crystallize from primary magmas of peridotite (black fields) that has been fertilized by 10 to 40% addition of a dacite melt (grey fields). Bold grey lines labeled OLLD are olivines that crystallize along a liquid line of descent at 0.2 GPa from a model peridotite that has been refertilized by 10% dacite; breaks in the OLLD at Mg-numbers of 82 and 80 represent clinopyroxene and plagioclase crystallization, respectively as indicated in Fig. 1. Model olivines are compared with observed Mangaia olivines from samples MGA-B-25, MGA-B-47, MG-1001, MG-1002 and those from Koolau and El Hierro (Sobolev et al., 2007; Gurenko et al., 2009). Fe/Mn is a ppm ratio.

silica-rich melt with olivine in peridotite. Fe/Mn in olivine is high because Mn is low owing to preferential partitioning into orthopyroxene. Ca decreases because the dacite composition and the variable mixtures are low in Ca. When the amount of dacite added to peridotite reaches about 40%, the mixture becomes nearly olivine-free pyroxenite and the olivines that crystallize from partial melts of this pyroxenite become similar in composition to many olivine phenocrysts from Koolau volcano in Hawaii and El Hierro in the Canary Islands (Fig. 3; Sobolev et al., 2007; Gurenko et al., 2009; Herzberg, 2011). The effect of including clinopyroxene and garnet in the pyroxenite residue would be to further increase Ni and Fe/Mn and decrease Ca, based on partition coefficients given in Herzberg et al. (2013).

A role for pyroxenite melting has been recognized for Koolau and El Hiero using a wide variety of geochemical, isotopic, and petrological approaches (Sobolev et al., 2007; Gurenko et al., 2009; Herzberg, 2011; Day et al., 2009, 2010; Hauri, 1996; Lassiter and Hauri, 1998; Blichert-Toft et al., 1999; Huang and Frey, 2005; Jackson et al., 2012). Melts of pyroxenite can be SiO_2-rich like Koolau and SiO_2-poor like El Hierro and Mangaia (Herzberg, 2011), and it is important to understand how they can be related. At high pressures the pyroxene-garnet plane is a thermal divide that separates SiO_2-rich and -poor pyroxenite, and it is not possible to derive a partial melt of one from the other. A typical basalt, for example, is SiO_2-rich and will consist of quartz or coesite eclogite which, when melted can produce dacitic SiO_2-rich melts. The following are different petrological pathways that can yield El Hierro- or Koolau-type basalts: 1) Dacitic melts can react with peridotite to make the second stage pyroxenite consisting of Cpx + Gt + Opx + Qz (quartz or coesite); partial melts are MgO- and SiO_2-rich basalts similar to Koolau primary magmas; they plot to the SiO_2-rich side of the pyroxene–garnet plane, or within the plane (Herzberg, 2011); olivine phenocrysts from such melts will have maximum Ni contents (Fig. 3). 2) The infiltration of low degree SiO_2-rich melts or advanced melts into surrounding peridotite will react with it, producing a refertilized peridotite which, when melted, can yield an SiO_2-poor alkali melt (Yaxley and Green, 1998); addition of CO_2 is expected to further lower SiO_2 (Dasgupta et al., 2007) and will likely contribute to the wide range of silica deficient rock types in the Canary and Cook–Austral Islands. 3) Bimineralic eclogite residues of advanced melts of the basalt protolith will be in spatial contact with peridotite, producing a local region of olivine-poor pyroxenite which can also yield SiO_2-poor melts (Herzberg, 2011). Olivine phenocrysts of refertilized peridotite can have high Ni, depending on the mass fraction of infiltrated SiO_2-rich melt (Fig. 3).

Mangaia lavas share the alkalic properties of El Hierro, and both have olivines with overlapping Ni at Mg-numbers in the 79–83 range. As discussed below, this might be evidence for a pyroxenite source origin for Mangaia. However, the evidence is contradictory in that Mangaia olivines exhibit an Ni trend towards those expected of a peridotite source but El Hierro does not. Mangaia Ca contents are similar to some olivines from El Hierro and fertilized peridotite, but others have much higher Ca contents and Mg-numbers (Fig. 3). Mangaia olivines have lower Fe/Mn than those expected of fertilized peridotite (Fig. 3), but this may be an artifact of spinel crystallization. The drop in Fe/Mn in El Hierro and Koolau is likely the result of spinel fractionation because spinel contains no Mn; its fractionation will drop Fe/Mn in the derivative magmas and the olivines from which they crystallize. For Mangaia, while the variation in Fe/Mn is within the precision of measurement, there is a hint of a refertilized peridotite source as seen by the distinct positive trend towards ~10% dacite addition (Fig. 3); the positive trend in Fe/Mn may be accounted for by some combination of olivine and spinel fractionation.

Olivine compositions for La Palma and La Gomera in the Canary Islands (Gurenko et al., 2009) shown in Fig. 4 are good examples of olivine crystallization from a refertilized peridotite source provenance. They are particularly helpful because the olivines extend to higher Mg-numbers than those from Mangaia, and provide a more secure inference about source lithology. For purposes of preserving clarity, we restrict this analysis to olivine populations with distinctive compositions; we have also excluded Mangaia samples, but the reader can readily draw

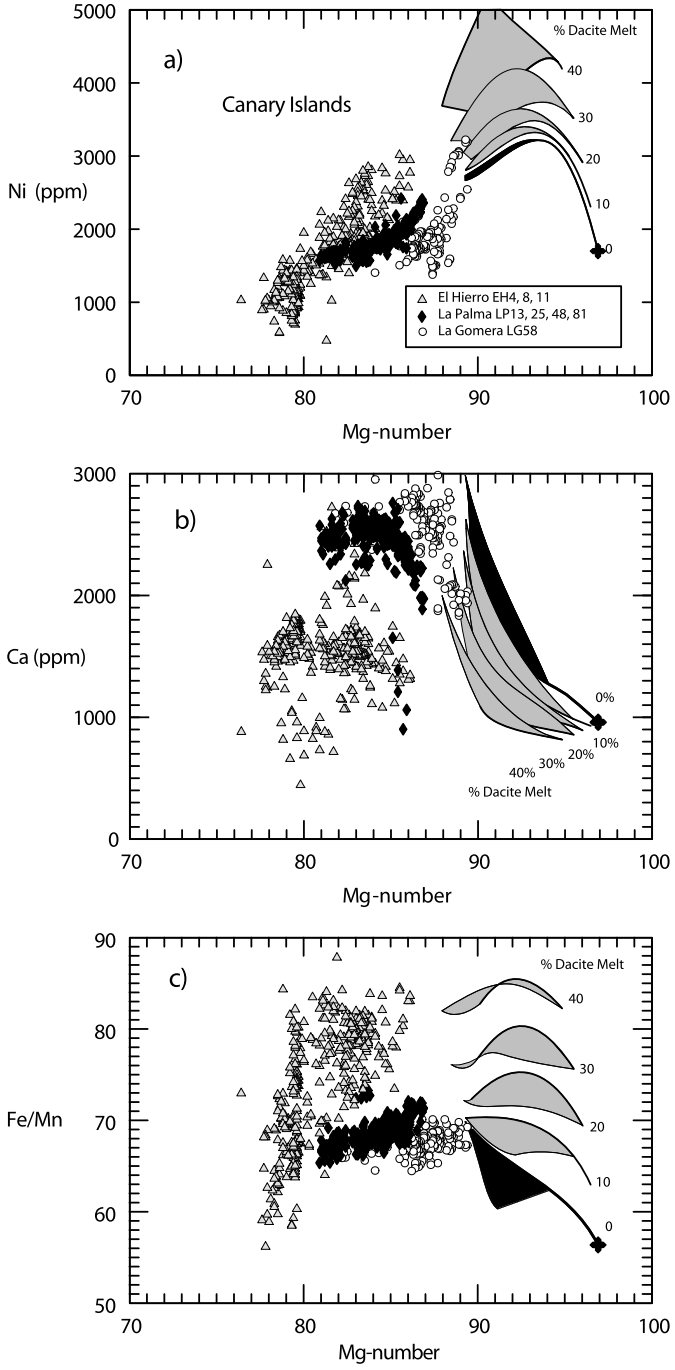

Fig. 4. A model of olivine compositions that crystallize from primary magmas of peridotite (black fields) that has been fertilized by variable addition of a dacite melt (grey fields), from Fig. 3, compared with selected olivines from the Canary Islands (Gurenko et al., 2009). Note the general compatibility between observed olivines from La Gomera and La Palma with model olivines of a peridotite source that has been fertilized with ~10–20% dacite melt. This is supporting evidence that Mangaia olivines having the highest Ca contents and Mg-numbers (Fig. 3) crystallized from a fertilized peridotite source, not pyroxenite. Fe/Mn is a ppm ratio.

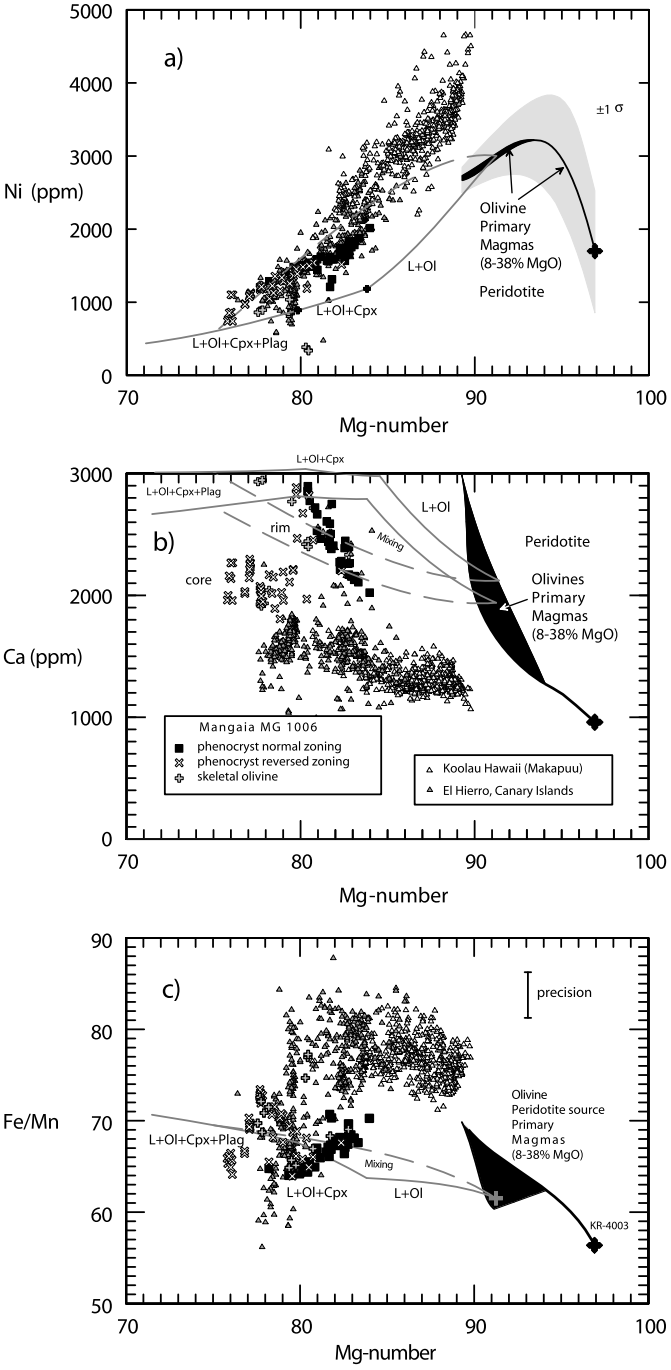

Fig. 5. Olivines from Mangaia sample MG-1006 compared with model olivines of a peridotite source (black fields), from Fig. 1. The solid gray lines are olivine compositions that crystallize from an assumed Mangaia primary magma that subsequently fractionated olivine, clinopyroxene and plagioclase at 0.2 GPa, an olivine liquid line of descent (OLLD). Core compositions of reversely zoned olivines, indicated by the white crosses, are similar to those from Koolau and El Hierro, for which a pyroxenite source was inferred (Sobolev et al., 2007; Gurenko et al., 2009). Rim compositions of reversely zoned olivines are similar to those of normally zoned olivines. Ca contents and Mg-numbers of normally zoned olivines, indicated by the black squares, trend in a direction towards olivines of a pyroxenite source provenance.

comparisons with Fig. 1. Many olivines from La Gomera have high Ca contents and Mg-numbers that are similar to Mangaia, and trend in a direction that is consistent with a peridotite that has been refertilized by about 10–20% dacite. Peridotite melting is most pronounced and yet, relative to other volcanoes in the Canary Islands, the lavas from La Gomera have the most radiogenic Sr, and Pb isotopic compositions (Gurenko et al., 2009).

6. Evidence for pyroxenite in the mantle source for Mangaia

Mangaia sample MG-1006 stands out as different from all others (Fig. 5). It is complex in that its olivines are both normally and inversely zoned in terms of Mg-number, it contains skeletal olivines, and large clinopyroxene phenocrysts that are spongy

and embayed. Zoning is more pronounced than for other Mangaia samples studied, and zoning profiles were obtained on 4 to 5 individual core-rim analyses without averaging. Reversely zoned olivines are generally larger than normally zoned olivines, and many are clearly separated from the normally zoned olivines in having anomalously low Ca and Mg-number. However, some of the reversely zoned grains trend towards the normally zoned population from core to rim, and develop high Ca contents characteristic of normally zoned olivines. A similar core-rim pattern is revealed in Fe/Mn (Fig. 5). Normally zoned olivines show a trend where Fe/Mn is positively correlated with Mg-number, reversely zoned olivines show a negative trend, and the two olivine populations converge at an Mg-number of about 80. We interpret these trends as olivines that crystallized from separate batches of magma that mixed; the reversely zoned olivines have compositions that are similar to many olivines from El Hierro. The normally zoned olivines have attributes of both peridotite and pyroxenite sources; the highest Ca contents and lowest Fe/Mn are similar to those of a peridotite source; however, in detail they define trends in the direction of olivines from Koolau volcano, and there is some overlap with olivines from El Hierro (Fig. 5). It is possible that the entire olivine population in MG-1006 originated from the mixing of separate batches of pyroxenite-source magmas. To relate them, it is likely that the early batch crystallized olivines with the lowest Mg-numbers settled as antecrysts in the next batch of magma, and partial reequilibration was expressed as reversed zoning along the rims.

It is notable that our inference for pyroxenite in sample MG-1006 may not be unique. It is also possible that they may be accidental olivines from a crystal mush in a magma chamber containing clinopyroxene, which acts to sequester Ca from the olivine. The exchange of Ca between olivine and clinopyroxene is well-documented in olivines from lithospheric peridotite that typically have $<$600 ppm Ca (De Hoog et al., 2010). Magma chamber recharge is consistent with reversely zoned olivines and clinopyroxenes that are spongy and embayed. This alternate interpretation would be consistent with a refertilized peridotite source for MG-1006, and may explain why all Mangaia samples have the same isotopic compositions.

7. Phantom, fugitive and possible stealth recycled crust as recorded in olivine chemistry

Fig. 6 captures the similarities and differences in olivine Ca contents for all Mangaia samples that were studied. Olivines from Mangaia samples MG-1001, MG-1002, MGA-B-25 and MGA-B-47 have Ca contents that are high and trend to high Mg-numbers characteristic of crystallization from derivative melts of peridotite or refertilized peridotite. If the isotopic compositions were inherited from subduction of recycled oceanic crust, then this crust can be considered phantom because its lithological identity has been destroyed. A mechanism for partial crust destruction that is compatible with the olivine chemistry has partial melting of recycled crust and metasomatic injection of silicic melts into the surrounding peridotite (Yaxley and Green, 1998; Spandler et al., 2008; Prytulak and Elliott, 2009; Day et al., 2009, 2010; Hanyu et al., 2011; Mallik and Dasgupta, 2012, 2013). For Mangaia, direct evidence for a role played by recycled crust is in olivine chemistry of sample MG-1006. Olivines in this sample can have lower Ca contents, and trend in directions that are consistent with a pyroxenite source. Given that the crustal lithological identity had successfully escaped destruction by partial melting, we refer to this as "fugitive" recycled crust.

For the entire olivine database with normal zoning, there is convergence to a common Ca content and Mg-number of $\sim$80 (Fig. 6); they are also similar in Fe/Mn and Ni (Figs. 1, 4). Clearly,

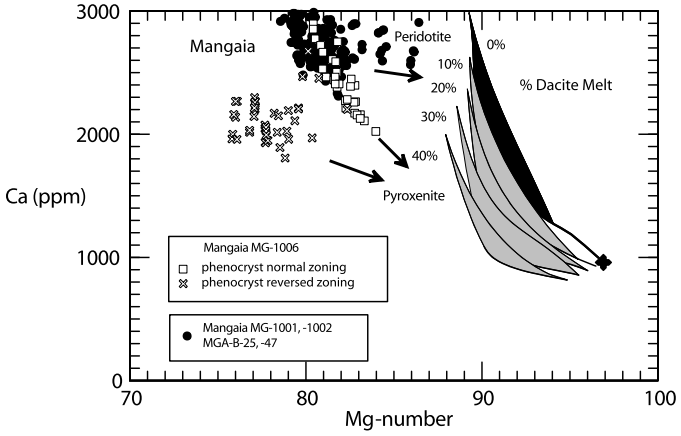

Fig. 6. Summary of Ca contents and Mg-numbers for all measured Mangaia olivine phenocrysts compared with olivines expected to crystallize from primary magmas of a peridotite source that had variable amounts of dacite added, from Fig. 3. Ca contents of observed olivine phenocrysts trend in directions that point towards fertilized peridotite and pyroxenite sources.

no inferences about source lithology would be secure from this population of data having a restricted composition. It is consistent with magma chamber fractional crystallization, recharge, and mixing of magmas of a variably fertilized peridotite source (Figs. 1, 3). But it may also be consistent with pyroxenite melts that undergo similar magma chamber processes; unfortunately, we cannot identify an appropriate lava composition for which a liquid line of decent can be computed. It is further conjectured that the convergent olivines may have crystallized from the mixing of peridotite- and pyroxenite-sources that fractionated to a common LLD. Whatever the correct explanation may be, it is clear that information concerning the source lithologies of primary magmas can be destroyed by both magma chamber and deep partial melting processes. If the details in our analysis of the problem seem unsatisfactory, they are given in the spirit of trying to give substance and definition to a phantom.

This analysis has been restricted to the formation of stage 2 pyroxenite and refertilized peridotite by dacitic melt production from recycled basalt. It is a successful way of explaining many petrological and geochemical features, but it may not be unique. High degree or total melts of a pyroxenite protolith with a basaltic composition must necessarily yield basaltic compositions, not dacite (Pertermann and Hirschmann, 2003; Spandler et al., 2008). Stage 2 pyroxenite that forms by reaction of basalt with peridotite will have lower Ni and higher Ca contents and higher Fe/Mn, as will their partial melts and crystallizing olivines (Herzberg, 2011). We term this class of pyroxenite as "stealth pyroxenite" in that it may melt and crystallize olivine phenocrysts with compositions similar to those of melts from mantle peridotite. And, it is expected to be similar to phantom pyroxenite in that it has the isotopic and geochemical characteristics of recycled crust, but olivine compositions with a peridotite source provenance. The possible formation of stealth pyroxenite requires further study from both a computational and experimental point of view. If verified, it will indicate that our interpretation of a refertilized source for Mangaia is not be unique and, most importantly, it would place important restrictions on the use of olivine chemistry to infer source lithology.

8. Source lithology–isotope relations

Our working hypothesis is a mixed peridotite and pyroxenite source for Mangaia, with peridotite dominating. However, we cautioned in Section 6 that the source may have consisted exclusively refertilized peridotite, and that our pyroxenite interpretation for sample MG-1006 may be compromised by Ca exchange

between olivine and clinopyroxene in a magma chamber. If Mangaia melted from a mixed peridotite–pyroxenite source, then some mechanism is required to account for the similarity in isotopic compositions for all samples studied. Isotopic homogeneity may arise owing to magma mixing and chemical exchange governed by solid-state diffusion or dissolution–precipitation mechanisms during melt transport by porous or channel flow (Hauri, 1997). We can imagine that fugitive pyroxenite might adopt the isotopic composition of the dominant matrix of refertilized peridotite and its partial melt by melt-rock reaction, but this conjecture would benefit from theoretical work. Analogue studies of pyroxenite contained in orogenic peridotite might be another avenue of study, but current studies reveal conflicting results, with lithological heterogeneity revealed in both isotopic homogeneity and heterogeneity (Santos et al., 2002; Pearson and Nowell, 2004; Brueckner et al., 2010).

9. Conclusions

Inferences have been drawn about possible mantle source lithologies that melted to yield lavas from Mangaia in the Cook–Austral island chain, Polynesia. The method involves a comparison of olivine phenocryst chemistry with forward calculations of olivine compositions that are expected to crystallize from primary magmas of peridotite that has been variably fertilized by a dacite melt produced by partial melting of pyroxenite. Olivine phenocrysts have Mg-numbers that are too low to have been direct precipitates from primary magmas, and inferences about source lithology require an evaluation of the effects of magma chamber fractional crystallization, recharge, and mixing. Results show that most olivine phenocrysts from Mangaia have Ni and Ca contents and Fe/Mn ratios that are consistent with crystallization of magmas that originated from a peridotite or fertilized peridotite source. If the isotopic compositions were inherited from subduction of recycled oceanic crust, then its lithological identity has been destroyed. A mechanism for partial crust destruction that is compatible with the olivine chemistry has partial melting of recycled crust and metasomatic injection of silicic melts into the surrounding peridotite (Yaxley and Green, 1998; Spandler et al., 2008; Prytulak and Elliott, 2009; Day et al., 2009, 2010; Hanyu et al., 2011). Direct evidence in support of this model has been found in olivines from one Mangaia sample that have preserved the chemical signature of pyroxenite. We conclude that the commonly used terms mantle “heterogeneities” and “streaks” are ambiguous, and distinction should be made of its lithological and isotopic properties.

Acknowledgements

We are grateful to anonymous reviewers and to Tim Elliott for comments. CH thanks Paul Asimow for help with pMELTS. MGJ acknowledges funding from OCE-1153894 and EAR-1145202. JMDD acknowledges support from NSF EAR-1116089 and the National Geographic Society (GEFNE28-11).

Appendix A. Supplementary material

Supplementary material related to this article can be found online at http://dx.doi.org/10.1016/j.epsl.2014.03.065.

References

Albarède, F., Luais, B., Fitton, G., Semet, M., Kaminski, E., Upton, B.G.J., Bachèlery, P., Cheminée, J.-L., 1997. The geochemical regimes of Piton de la Fournaise volcano (Réunion) during the last 530 000 years. J. Petrol. 38, 171–201.

Beattie, P., Ford, C., Russell, D., 1991. Partition coefficients for olivine-melt and orthopyroxene-melt systems. Contrib. Mineral. Petrol. 109, 212–224.

Blichert-Toft, J., Frey, F.A., Albarède, F., 1999. Hf isotope evidence for pelagic sediments in the source of Hawaiian basalts. Science 285, 879–882.

Boyd, F.R., Mertzman, S.A., 1987. Composition and structure of the Kaapvaal lithosphere, southern Africa. In: Mysen, B.O. (Ed.), Magmatic Processes: Physicochemical Principles. In: Geochim. Soc. Spec. Publ., vol. 1, pp. 13–24.

Brueckner, H.K., Carswell, D.A., Griffin, W.L., Medaris Jr., L.G., Van Roermund, H.L.M., Cuthbert, S.J., 2010. The mantle and crustal evolution of two garnet peridotite suites from the Western Gneiss Region, Norwegian Caledonides: an isotopic investigation. Lithos 117, 1–19.

Cabral, R., Jackson, M.G., Rose-Koga, E.F., Koga, K.T., Whitehouse, M.J., Antonelli, M.A., Farquhar, J., Day, J.M.D., Hauri, E.H., 2013. Anomalous sulphur isotopes in plume lavas reveal deep mantle storage of Archaean crust. Nature 496, 490–493.

Chauvel, C., Hofmann, A., Vidal, P., 1992. HIMU-EM: the French Polynesian connection. Earth Planet. Sci. Lett. 110, 99–119.

Chauvel, C., Goldstein, S.L., Hofmann, A.W., 1995. Hydration and dehydration of oceanic crust controls Pb evolution in the mantle. Chem. Geol. 126, 65–75.

Chauvel, C., McDonough, W., Guille, G., Maury, R., Duncan, R., 1997. Contrasting old and young volcanism in Rurutu Island, Austral chain. Chem. Geol. 139, 125–143.

Danyushevsky, L.V., 2001. The effect of small amounts of H_2O on crystallisation of mid-ocean ridge and backarc basin magmas. J. Volcanol. Geotherm. Res. 110, 265–280.

Danyushevsky, L.V., Plechov, P., 2011. Petrolog3: integrated software for modeling crystallization processes. Geochem. Geophys. Geosyst. 12, Q07021. http://dx.doi.org/10.1029/2011GC003516.

Dasgupta, R., Hirschmann, M.M., Smith, N.D., 2007. Partial melting experiments of peridotite CO_2 at 3 GPa and genesis of alkalic ocean island basalts. J. Petrol. 48, 2093–2124.

Day, J.M.D., Pearson, D.G., Macpherson, C.G., Lowry, D., Carracedo, J.L., 2009. Pyroxenite-rich mantle formed by recycled oceanic lithosphere: oxygen–osmium isotope evidence from Canary Island lavas. Geology 37, 555–558.

Day, J.M.D., Pearson, D.G., Macpherson, C.G., Lowry, D., Carracedo, J.C., 2010. Evidence for distinct proportions of subducted oceanic crust and lithosphere in HIMU-type mantle beneath El Hierro and La Palma, Canary Islands. Geochim. Cosmochim. Acta 74, 6565–6589.

Day, J.M.D., Hilton, D.R., 2011. Origin of $^3He/^4He$ ratios in HIMU-type basalts constrained from Canary Island lavas. Earth Planet. Sci. Lett. 305, 226–234.

De Hoog, J.C.M., Gall, L., Cornell, D.H., 2010. Trace-element geochemistry of mantle olivine and application to mantle petrogenesis and geothermobarometry. Chem. Geol. 270, 196–215.

Donovan, J.J., 2012. Probe for EPMA: Acquisition, Automation and Analysis, Enterprise Edition. Probe Software, Inc., Eugene.

Dupuy, C., Barsczus, H.G., Dostal, J., Vidal, P., Liotard, J.-M., 1989. Subducted and recycled lithosphere as the mantle sources of ocean island basalts from Southern Polynesia, Central Pacific. Chem. Geol. 77, 1–18.

Geist, D., Naumann, T., Larson, P., 1998. Evolution of Galapagos magmas: mantle and crustal fractionation without assimilation. J. Petrol. 39, 953–971.

Ghiorso, M.S., Hirschmann, M.M., Reiners, P.W., Kress, V.C., 2002. The pMELTS: a revision of MELTS for improved calculation of phase relations and major element partitioning related to partial melting of the mantle to 3 GPa. Geochem. Geophys. Geosyst. 3. http://dx.doi.org/10.1029/2001GC000217.

Gurenko, A., Sobolev, A.V., Hoernle, K.A., Hauff, F., Schmincke, H.-U., 2009. Enriched, HIMU-type peridotite and depleted recycled pyroxenite in the Canary plume: a mixed-up mantle. Earth Planet. Sci. Lett. 277, 514–524.

Gurenko, A., Hoernle, K.A., Sobolev, A.V., Hauff, F., Schmincke, H.-U., 2010. Source components of the Gran Canaria (Canary Islands) shield stage magmas: evidence from olivine composition and Sr–Nd–Pb isotopes. Contrib. Mineral. Petrol. 159, 689–702.

Hanyu, T., Tatsumi, Y., Senda, R., Miyazaki, T., Chang, Q., Hirahara, Y., Takahashi, T., Kawabata, H., Suzuki, K., Kimuria, J.-I., 2011. Geochemical characteristics and origin of the HIMU reservoir: a possible mantle plume source in the lower mantle. Geochem. Geophys. Geosyst. 12, Q0AC09. http://dx.doi.org/10.1029/2010GC003252.

Hart, S.R., Davis, K.E., 1978. Nickel partitioning between olivine and silicate melt. Earth Planet. Sci. Lett. 40, 203–219.

Hauri, E.H., 1996. Major-element variability in the Hawaiian mantle plume. Nature 382, 415–419.

Hauri, E.H., 1997. Melt migration and mantle chromatography, 1: simplified theory and conditions form chemical and isotopic decoupling. Earth Planet. Sci. Lett. 153, 1–19.

Hauri, E., Hart, S.R., 1993. Re–Os isotope systematic of HIMU and EMII oceanic island basalts from the south Pacific Ocean. Earth Planet. Sci. Lett. 114, 353–371.

Hauri, E., Hart, S.R., 1997. Rhenium abundances and systematic in oceanic basalts. Chem. Geol. 139, 185–205.

Herzberg, C., 2011. Identification of source lithology in the hawaiian and Canary Islands: implications for origins. J. Petrol. 52, 113–146.

Herzberg, C., Asimow, P.D., 2008. Petrology of some oceanic island basalts: PRIMELT2.XLS software for primary magma calculation. Geochem. Geophys. Geosyst. 8, Q09001. http://dx.doi.org/10.1029/2008GC002057.

Herzberg, C., Gazel, E., 2009. Petrological evidence for secular cooling in mantle plumes. Nature 458, 619–622.
Herzberg, C., O'Hara, M.J., 2002. Plume-associated ultramafic magmas of Phanerozoic age. J. Petrol. 43, 1857–1883.
Herzberg, C., Asimow, P., Ionov, D., Vidito, C., Jackson, M.G., Geist, D., 2013. Nickel and helium evidence for melt above the core-mantle boundary. Nature 493, 393–397.
Hofmann, A.W., 1997. Mantle geochemistry: the message from oceanic volcanism. Nature 385, 219–229.
Hofmann, A.W., White, W.M., 1982. Mantle plumes from ancient oceanic crust. Earth Planet. Sci. Lett. 57, 421–436.
Huang, S., Frey, F.A., 2005. Recycled oceanic crust in the Hawaiian plume: evidence from temporal geochemical variations within the Koolau shield. Contrib. Mineral. Petrol. 149, 556–575.
Jackson, M.G., Hart, S.R., Saal, A.E., Shimizu, N., Kurz, M.D., Blusztajn, J., Skovgaard, A., 2008. Globally elevated titanium, tantalum, and niobium (TITAN) in ocean island basalts with high $^{3}He/^{4}He$. Geochem. Geophys. Geosyst. 9. http://dx.doi.org/10.1029/2007GC001876.
Jackson, M.G., Dasgupta, R., 2008. Compositions of HIMU, EM1, and EM2 from global trends between radiogenic isotopes and major elements in ocean island basalts. Earth Planet. Sci. Lett. 276, 175–186.
Jackson, M.G., Weis, D., Huang, S., 2012. Major element variations in Hawaiian shield lavas: source features and perspectives from global ocean island basalt (OIB) systematics. Geochem. Geophys. Geosyst. 13, Q09009. http://dx.doi.org/10.1029/2012GC004268.
Jones, J.H., 1984. Temperature and pressure-independent correlations of olivine-liquid partition coefficients and their application to trace element partitioning. Contrib. Mineral. Petrol. 88, 126–132.
Kelemen, P.B., Hart, S.R., Bernstein, S., 1998. Silica enrichment in the continental upper mantle via melt/rock reaction. Earth Planet. Sci. Lett. 164, 387–406.
Kelley, K.A., Plank, T., Farr, L., Ludden, J., Staudigel, H., 2005. Subduction cycling of U, Th, and Pb. Earth Planet. Sci. Lett. 234, 369–383.
Kogiso, T., Tatsumi, Y., Shimoda, G., Barsczus, H.G., 1997. High μ (HIMU) ocean island basalts in southern Polynesia: new evidence for whole mantle scale recycling of subducted oceanic crust. J. Geophys. Res. 102, 8085–8103.
Lange, R.A., Carmichael, I.S.E., 1987. Densities of Na_2O–K_2O–CaO–MgO–FeO–Fe_2O_3–Al_2O_3–TiO_2–SiO_2 liquids: new measurements and derived partial molar properties. Geochim. Cosmochim. Acta 51, 2931–2946.
Lassiter, J.C., Hauri, H., 1998. Osmium-isotope variations in Hawaiian lavas: evidence for recycled oceanic lithosphere in the Hawaiian plume. Earth Planet. Sci. Lett. 164, 483–496.
Le Roux, V., Dasgupta, R., Lee, C.-T.A., 2011. Mineralogical heterogeneities in the Earth's mantle: Constraints from Mn, Co, Ni and Zn partitioning during partial melting. Earth Planet. Sci. Lett. 307, 395–408.
Li, C., Ripley, E.M., 2010. The relative effects of composition and temperature on olivine–liquid Ni partitioning: statistical deconvolution and implications for petrologic modeling. Chem. Geol. 275, 99–104.
Liu, Y., Gao, S., Lee, C.-T., Hu, S., Liu, X., Yuan, H., 2005. Melt-peridotite interactions: links between garnet pyroxenite and high-Mg# signature of continental crust. Earth Planet. Sci. Lett. 234, 39–57.
Mallik, A., Dasgupta, R., 2012. Reaction between MORB-eclogite derived melts and fertile peridotite and generation of ocean island basalts. Earth Planet. Sci. Lett. 329–330, 97–108.
Mallik, A., Dasgupta, R., 2013. Reactive infiltration of MORB-eclogite-derived carbonated silicate melt into fertile peridotite at 3 GPa and genesis of alkalic magmas. J. Petrol. 54, 2267–2300.
Marchesi, C., Garrido, C.J., Bosch, D., Bodinier, J.-L., Gervilla, F., Hidas, K., 2013. Mantle refertilization by melts of crustal-derived garnet pyroxenite: evidence from the Ronda peridotite massif, southern Spain. Earth Planet. Sci. Lett. 362, 66–75.
Matzen, A.K., Baker, M.B., Beckett, J.R., Stolper, E.M., 2013. The temperature and pressure dependence of nickel partitioning between olivine and silicate melt. J. Petrol. 54, 2521–2545.
Morgan, W.J., 1971. Convection plumes in the lower mantle. Nature 230, 42–43.
Niu, Y., Wilson, M., Humphreys, E.R., O'Hara, M.J., 2011. The origin of intra-plate ocean island basalts (OI B): the lid effect and its geodynamic implications. J. Petrol. 52, 1443–1468.
O'Hara, M.J., 1968. The bearing of phase equilibria studies in synthetic and natural systems on the origin of basic and ultrabasic rocks. Earth-Sci. Rev. 4, 69–133.
O'Hara, M.J., 1977. Geochemical evolution during fractional crystallization of a periodically refilled magma chamber. Nature 266, 503–507.
O'Neill, H.St.C., Jenner, F., 2012. The global pattern of trace-element distributions in ocean floor basalts. Nature 491, 698–704.
Parai, R., Mukhopadhyay, S., Lassiter, J., 2009. New constraints on the HIMU mantle from neon and helium isotopic compositions of basalts from the Cook–Austral Islands. Earth Planet. Sci. Lett. 277, 253–261.
Pearson, D.G., Nowell, G.M., 2004. Re–Os and Lu–Hf isotope constraints on the origin and age of pyroxenites from the Beni Bousera peridotite massif: implications for mixed peridotite–pyroxenite mantle sources. J. Petrol. 45, 439–455.
Pertermann, M., Hirschmann, M.M., 2003. Anhydrous partial melting experiments on MORB-like eclogite: phase relations, phase compositions and mineral-melt partitioning of major elements at 2–3 GPa. J. Petrol. 44, 2173–2201.
Prytulak, J., Elliott, T., 2007. TiO_2 enrichment in ocean island basalts. Earth Planet. Sci. Lett. 263, 388–403.
Prytulak, J., Elliott, T., 2009. Determining melt productivity of mantle source from ^{238}U–^{230}Th and ^{235}U–^{231}Pa disequilibria: an example from Pico Island, Azores. Geochim. Cosmochim. Acta 73, 2103–2122.
Putirka, K.D., Ryerson, F.J., Perfit, M., Ridley, W.I., 2011. Mineralogy and composition of oceanic mantle. J. Petrol. 52, 279–313.
Saal, A.E., Hart, S.R., Shimizu, N., Hauri, E.H., Layne, G.D., 1998. Pb isotopic variability in melt inclusions from ocean island basalts, Polynesia. Science 282, 1481–1484.
Santos, J.F., Schärer, U., Gil Ibarguchi, J.I., Girardeau, J., 2002. Genesis of pyroxenite-rich peridotite and Cabo Ortegal (NW Spain): geochemical and Pb–Sr–Nd isotope data. J. Petrol. 43, 17–43.
Sobolev, A.V., Hofmann, A.W., Sobolev, S.V., Nikogosian, I.K., 2005. An olivine-free mantle source of Hawaiian shield basalts. Nature 434, 590–597.
Sobolev, A.V., Hofmann, A.W., Kuzmin, D.V., Yaxley, G.M., Arndt, N.T., Chung, S.-L., Danyushevsky, L.V., Elliott, T., Frey, F.A., Garcia, M.O., Gurenko, A.A., Kamenetsky, V.S., Kerr, A.C., Krivolutskaya, N.A., Matvienkov, V.V., Nikogosian, I.K., Rocholl, A., Sigurdsson, I.A., Sushchevskaya, N.M., Teklay, M., 2007. The amount of recycled crust in sources of mantle-derived melts. Science 316, 412–417.
Spandler, C., Yaxley, G., Green, D.H., Rosenthal, A., 2008. Phase relations and melting of anhydrous K-bearing eclogite from 1200 to 1600 °C and 3 to 5 GPa. J. Petrol. 49, 771–795.
Vidito, C., Herzberg, C., Gazel, E., Geist, D., Harpp, K., 2013. Lithological structure of the Galápagos Plume. Geochem. Geophys. Geosyst. 14. http://dx.doi.org/10.1002/ggge.20270.
Walter, M.J., 1998. Melting of garnet peridotite and the origin of komatiite and depleted lithosphere. J. Petrol. 39, 29–60.
Wang, Z., Gaetani, G.A., 2008. Partitioning of Ni between olivine and siliceous eclogite partial melt: experimental constraints on the mantle source of Hawaiian basalts. Contrib. Mineral. Petrol. 156, 661–678.
Weaver, B., 1991. The origin of ocean island basalt end-member compositions: trace element and isotopic constraints. Earth Planet. Sci. Lett. 104, 381–397.
White, W.M., Hofmann, A.W., 1982. Sr and Nd isotope geochemistry of oceanic basalts and mantle evolution. Nature 296, 821–825.
Willbold, M., Stracke, A., 2006. Trace element composition of mantle end-members: implications for recycling of oceanic and upper and lower continental crust. Geochem. Geophys. Geosyst. 7, Q04004. http://dx.doi.org/10.1029/2005GC001005.
Wood, C.P., 1978. Petrology of Atiu and Mangaia, Cook Islands (Note), N.Z. J. Geol. Geophys. 21, 767–771.
Woodhead, J.D., 1996. Extreme HIMU in an oceanic setting: the geochemistry of Mangaia Island (Polynesia), and temporal evolution of the Cook–Austral hotspot. J. Volcanol. Geotherm. Res. 72, 1–19.
Yaxley, G.M., Green, D.H., 1998. Reactions between eclogite and peridotite: mantle refertilisation by subduction of oceanic crust, Schweiz. Mineral. Petrogr. Mitt. 78, 243–255.
Zindler, A., Hart, S., 1986. Chemical geodynamics. Annu. Rev. Earth Planet. Sci. 14, 493–571.